TSINGHUA SCIENCE AND TECHNOLOGY
ISSN 1007-0214 15/18 pp233-240
Volume 11, Number 2, April 2006

Sol-Gel Synthesized Adsorbents for Metal Separation*

L. L. Tavlarides**, J. S. Lee, K. H. Nam, N. Agarwal

**Department of Chemical Engineering and Materials Science,
Syracuse University, Syracuse, NY 13244, USA**

Abstract: A series of organo-ceramic adsorbents have been synthesized by a sol-gel processing technique for metal ion extraction. These adsorbents generally have significantly high metal uptake capacities, good physical-chemical stabilities, and well-designed pore geometries compared to other pre-existing metal-chelating ceramic-based adsorbents. This work describes the synthesis and evaluation of pyrazole and calix[4]arene crown adsorbents for selective separation of platinum, palladium, and gold and cesium ions, respectively, from solutions. These materials exhibit mesoporous properties with high surface areas and pore volumes. The sol-gel synthesis starting with precursor silanes and titania results in gel particles of desired pore characteristics and high capacity and stability. Characterization studies, such as adsorption isotherms, breakthrough curves for fixed bed operation, and material stability, show promising results for applications to metal sepation.

Key words: metal separation; organo-ceramic adsorbent; calix[4]arene; sol-gel synthesis; mesoporous

Introduction

Noble nanostructured adsorbents are of emerging interest due to the ability to fabricate and control the chemical and physical properties of these materials. Numerous materials have been developed in attempts to separate metal ions from aqueous streams. Such efforts include improving the physicochemical properties and sorption efficiencies of the materials by fabricating pore geometries to improve mass transfer rates and separation efficiencies. Since the discovery of MCM-41[1], the ordered mesoporous molecular sieves, various functional groups have been immobilized on pore surfaces of similarly prepared materials for use as adsorbents[2-6]. These materials exhibit high ligand densities and good adsorption of metal ions from aqueous solutions. However, upon immobilization of functional groups on these well-defined pore surfaces, loss of surface area and reduction of pore diameter and pore volume can occur.

Studies[7,8] have shown that the loss of pore volume can be as high as 60%-84%. The degree of pore volume reduction could be a result of the nature of the ligand, such as the size and the ligand loading. Moreover, a comparative study[8] indicates that materials prepared by the immobilization method appear to have nonuniformly distributed functional groups, whereas the materials prepared by the sol-gel method appear to have uniformly distributed functional groups. Studies[9-12] have shown that by employing the sol-gel method with appropriate synthesis conditions, the resulting adsorbents can have high ligand densities and long life cycles[11].

We have developed a new approach of sol-gel syntheses of functional ceramics of OCAs (Fig. 1). The fundamental design of the synthesis is to independently hydrolyze and homo-condense the functional precursor

Received: 2005-10-09

* Supported by the National Science Foundation (Nos. CTS-9805118 and CTS-0120204)

** To whom correspondence should be addressed.
E-mail: lltavlar@syr.edu

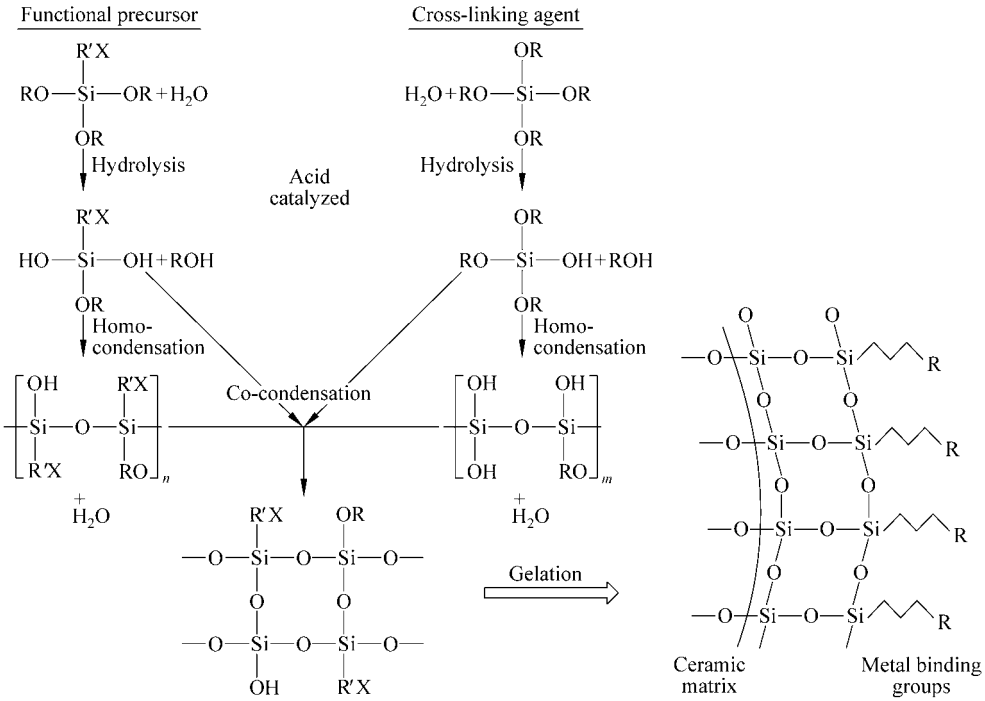

Fig. 1 Schematic synthesis route of OACs via sol-gel processing.

silanes (FPS) and cross-linking agent (CA) at desired reaction times to control the extent of oligomerizations. This synthesis pathway also provides the capability of maximizing the ligand density while maintaining structural rigidity and mesopores.

Using this approach, a series of organo-ceramic adsorbents have been synthesized for metal extractions in our laboratories[7-9]. These adsorbents generally have significantly high metal uptake capacities, good physico-chemical stabilities, and well-defined pore geometries compared to other pre-existing metal chelating ceramic-based adsorbents.

In this paper, we will examine two sorbent systems. The first group are pyrazole-functionalized organo-ceramic adsorbents (SOL-PzPs) for the extraction and separation of palladium(II), platinum(IV), and gold(III) chlorides from HCl solutions. Pyrazole compounds have been considered to be good metal chelants because of the nucleophilicity of nitrogen atoms, different steric accessibility through appropriate substitution, and hydrolytic and thermal stability[13]. Depending on the types of substituted ligands on the pyrazole moiety and the substitution positions, pyrazole functionalized compounds have different behavior in coordination with metal ions. Accordingly, these ligands have been utilized for metal complexations in many applications[14,15]. In particular, pyrazole-functionalized extractants have a good reactivity and selectivity for platinum group metals (PGM) over other transition metals[16-18].

The second group are calix[4]arene crown functional ceramics synthesized and employed to demonstrate selective encapsulation of cesium ions from simulants of DOE nuclear wastes. Both silica- and titania-based organo-ceramic adsorbents have been synthesized through sol-gel processing to have mesopores with ceramic frameworks. These materials are tested through batch and column experiments using highly acidic and alkaline solutions to show chemical stability and feasibility of selective separation.

1 Experimental

1.1 Pyrazole functionalized organo-ceramic adsorbents for noble metal separation

The functional precursor silane, N-(trimethoxysilylpropyl)-pyrazole (PzPs) is synthesized by the N-alkylation reaction using equimolar amounts of 1H-pyrazole (Lancaster Co.) and 3-chloropropyltrimethoxysilane (Aldrich Chemical Co.) in the presence of diisopropyl-ethylamime (Aldrich Chemical Co.) as a proton scavenger. The purity of PzPs used for adsorbent synthesis is more than 98% as determined by

GC/MS analysis.

The metal concentrations are measured with an atomic absorption spectrophotometer (Perkin-Elmer Model 2380) and an ICP-OES (Perkin-Elmer OPTIMA 3300DV). The average pore size and surface areas of the adsorbents are measured by nitrogen adsorption at 77 K with Micromeritics ASAP2000. Carbon and nitrogen contents of synthesized adsobents are measured by the elemental analysis.

Maximum uptake capacities for Pd(II), Pt(IV), and Au(III) chlorides at various HCl concentrations are measured by equilibrating a desired amount of the adsorbent (0.1-0.25 g) with 7-10 mmol/L of the metal chloride solutions at 25℃. For equilibrium adsorption isotherms, desired amounts of the adsorbent are equilibrated with the metal chloride solutions at 2.0 mol/L HCl concentration.

Metal uptake rates of SOL-PzPs-BD-5 are measured for Pd(II) chloride in a batch recycle reactor consisting of a 1.0-cm ID column containing 0.20 g of the adsorbent packed between two layers of 100-120 mesh glass beads. Prior to contact with the metal solutions, 200 mL of 2.0 mol/L HCl solution is circulated at 10 mL/min flow rate for at least 5 h to ensure complete wetting and protonation of the packed adsorbent.

Breakthrough experiments are performed with SOL-PzPs-BD-5 for Pd(II), Pt(IV), and Au(III) chlorides. For each breakthrough experiment, 2.0 g of SOL-PzPs-BD-5 are packed in a 0.8-cm ID column. Each feed solution contains approximately 1.0 mmol/L of one of the metal chlorides at 2.0 mol/L HCl concentration. The solutions are passed through the column at 1.0 mL/min flow rate and the effluent solutions are collected fractionally. When the column is saturated, the column is washed with 10 mL of water and stripped with 0.1 mol/L HCl solutions containing 0.5 mol/L thiourea for Pd(II) and Pt(IV) and 0.25 mol/L thiourea for Au(III) by passing at a flow rate of 1.0 mL/min.

1.2 Calix[4]arene crown functionalized organo-ceramic adsorbents for cesium separation

The calix[4]arene crown functional materials are synthesized by co-condensing cross linking agents with calix[4]arene crown functional precursor silanes under an acid catalyst. The synthesis of calix[4]arene derivative precursor silanes are based on the procedures reported in Refs. [19-21] and modified to produce the calix[4]arene-crown-6 FPS and calix[4]arene-benzocrown-6 FPS. The cross linking agents used are tetraethoxysilane (TEOS) and tetraisopropoxytitanate (TiPOT). The sol-gel synthesis procedure employed follows our sol-gel reaction scheme developed earlier[9]. The silica-based materials are named Calixol and CalixBC for calix[4]arene-crown-6 and calix[4]arene-benzocrown-6 functionalities, respectively, and the titania-based materials are named CC-Ti and CBC-Ti for calix[4]arene-crown-6 and calix[4]arene-benzocrown-6 functionalities.

Equilibrium adsorption experiments are conducted in batch modes at 1 mol/L HNO_3 by contacting an adsorbent amount of 0.1 g with 5 mL of cesium solution of various initial concentrations for 24 h at 25℃.

The stability of titania-based materials to withstand high alkaline conditions are tested by contacting the materials in a 2-mol/L NaOH solution for a continuous period of 8 days. The materials are filtered using a glass frit filter unit, washed with DI water and acetone several times, and dried in an oven at 80℃. The materials are then batch contacted with cesium solutions and the solution concentrations before and after contact are measured.

Column adsorption performance is investigated by flowing 1 L of 10 mg/L cesium solution through a 0.7-cm ID column packed with 0.45 g of adsorbent (particle size range is 125-180 μm) at a flow rate of 0.28 mL/min using a multi-cartridge peristaltic pump. Glass beads are placed at both ends of the adsorbent bed to ensure even flow of solution. The effluents from the column are collected for analyses of cesium concentrations. The bed capacity is calculated from the mass balance difference between the initial and the total effluent solutions.

2 Results and Discussion

2.1 Pyrazole functionalized organo-ceramic adsorbents for noble metal separation

The organo-ceramic adsorbents, with and without hydrothermal treatment, SOL-PzPs-BD-5 and SOL-PzPs-B-18, respectively, have different metal uptake capacities, pore characteristics, and adsorption properties even though these materials are from the same batch. Accordingly, it is of interest to determine how

the hydrothermal treatment alters the material properties and adsorption characteristics.

As shown in Table 1, both the carbon and the nitrogen contents of SOL-PzPs-B-18 decrease after the hydrothermal treatment (SOL-PzPs-BD-5). This result indicates that the adsorbent structure may be broken down, the unbounded fraction of adsorbent is leached, or both of these occur simultaneously during the treatment. In addition, the increase of pore volume after the treatment supports the loss of part of the adsorbent. However, it is observed that the Pd(II) uptake capacities of SOL-PzPs-B-18 and SOL-PzPs-BD-5 are the same in 2.0 mol/L HCl solutions, regardless of the loss in ligand density.

Table 1 Physico-chemical characteristics of SOL-PzPs-B-18 and SOL-PzPs-BD-5

Adsorbent	Elemental Analysis		Ligand density*	$q_{Pd}(II)^{**}$/	Pore characteristics		
	C (wt.%)	N (wt.%)	(mmol/g)	(mmol • g^{-1})	D/nm	SA(m^2/g)	V_P/(cm^3 • g^{-1})
B-18	23.9	9.3	3.3	1.40±0.01	3.7	124	0.13
BD-5	22.7	8.8	3.1	1.41±0.05	3.7	437	0.40

* From C and N elemental analyses; ** Palladium uptake capacity at 2.0 mol/L HCI concentration.

The experimental results for equilibrium uptake capacities of SOL-PzPs-BD-5 in 2.0 mol/L HCl solutions show that this adsorbent has substantially higher Pd(II) uptake capacity than that for Pt(IV) and Au(III) at low metal concentrations (Fig. 2). The adsorbent is almost saturated with approximately 0.2 mmol/L of Pd(II) chloride at equilibrium in the solution but is not completely saturated either by Pt(IV) or Au(III) chlorides even at 3 mmol/L or more metal concentrations. The differences of equilibrium uptake capacities for these three metal chlorides indicate that this adsorbent has stronger affinity for Pd(II) chloride over Pt(IV) and Au(III) chlorides and provides a utility for almost complete separation of palladium over the others. Based on the proton pairing reactions of the metal-chloride ions, $PdCl_4^{2-}$, $PdCl_6^{2-}$, and $AuCl_4^-$ for Pd(II), Pt(IV), and Au(III) and this adsorbent, the isotherms can be described with bi- and mono-adsorption mechanisms. To avoid complicated mathematical description for the bi-adsorption, it is assumed that Pd(II) and Pt(IV) chlorides quasi-mono-dentate complexes react with clusters of two ligands, whereas one Au(III) chloride ion reacts with one ligand.

The adsorption mechanism for Pd(II), Pt(IV), and Au(III) chlorides can be rewritten based on these assumption as

$$MCl_n^{-(n-m)} + \overline{(RNH^+)_{n-m}} \leftrightarrow \overline{MCl_n(RNH)_{n-m}} \qquad (1)$$

where $\overline{(RNH^+)_{n-m}}$ is considered to be a cluster of $n-m$ number of protonated pyrazole moieties for Pd(II) and Pt(IV) chlorides or a single protonated pyrazole ligand for Au(III) chloride.

The adsorption equilibrium isotherms for these metal chlorides can be described with a modified Langmuir isotherm:

$$q_i = \frac{K_i Q f_i C_i}{1 + K_i C_i} \qquad (2)$$

where q_i is the adsorbed amount of metal i (mmol/g); Q is the ligand density (3.1 mmol/g); f_i is the correction factor for actual maximum uptake with respect to the ligand density; K_i is the isotherm constant for metal chloride i; C_i is the concentration of metal i; and i is Pd(II), Pt(IV), or Au(III).

These Langmuir type adsorption isotherms are fitted to experimental equilibrium data at 2.0 mol/L HCl concentrations to find the isotherm constants (K_i) and the correction parameters (f_i). With the fitting parameters given in Table 2, the experimental equilibrium data are well represented as shown in Fig. 2. The correction parameters (f_i) are the ratios of actual maximum uptake capacities with respect to the ligand density. If the adsorption reactions of Pd(II), Pt(IV), and Au(III) chlorides with pyrazole ligands occur as proposed (Eq. (1)), the f values should be 0.5, 0.25, and 1.0, respectively. However, the fitted values of f are smaller than these ideal values. These differences between the ideal values and fitted values are due to high HCl concentrations in solutions at which the adsorbent interacts not only with these metal chlorides but also with free chlorides.

Among the three metal chloride systems, the Pd(II) chloride system is employed to study the adsorption

Table 2 Langmuir isotherm constant (*K*) and effectiveness factor (*f*) for adsorption uptake capacity

Species	*K*	*f*
$PdCl_4^{2-}$	15.56±7.91	0.447±0.005
$PtCl_6^{2-}$	0.56±0.17	0.248±0.033
$AuCl_4^-$	0.36±0.04	0.800±0.035

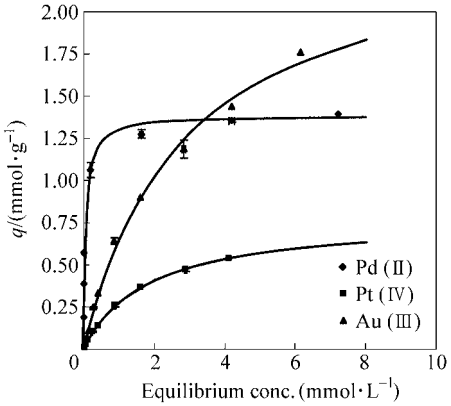

Fig. 2 Equilibrium adsorption isotherms of SOL-PzPs for Pd(II) (◆), Pt(IV) (■), and Au(III) (▲) chlorides at [HCl] = 2.0 mol/L.

kinetics of SOL-PzPs-BD-5 because this adsorbent has the strongest selectivity for Pd(II) chloride over Pt(IV) and Au(III) chlorides. The results from these experiments show that the apparent adsorption kinetics are affected by the particle size and that the diffusion of Pd(II) chloride ions in pores controls the adsorption process. We therefore employed a pore diffusion model to predict the adsorption of Pd(II) chlorides using on SOL-PzPs-BD-5. Experimental and calculated results for adsorption in a batch recycle reactor are shown in Fig. 3.

The adsorption behavior of SOL-PzPs-BD-5 in a packed column is studied for Pt(IV), Au(III), and Pd(II) chlorides by performing individual breakthrough experiments at 1.0 mmol/L concentration of each of these metal chlorides in 2.0 mol/L HCl solutions.

The experimental results show that the breakthroughs occur in sequence of Pd(II), Pt(IV), and Au(III) chlorides as shown in Fig. 4. Two consecutive breakthroughs occur for the platinum chloride system after 25 bed volumes (0.07 L) for which C/C_0 remains at 0.1 until 180 bed volumes (0.54 L) at which the main breakthrough occurs. A similar phenomenon is also observed for the feed concentration of 1.53 mmol/L at 2.0 mol/L HCl concentration, in which case C/C_0 remains at 0.085 before the second breakthrough occurs.

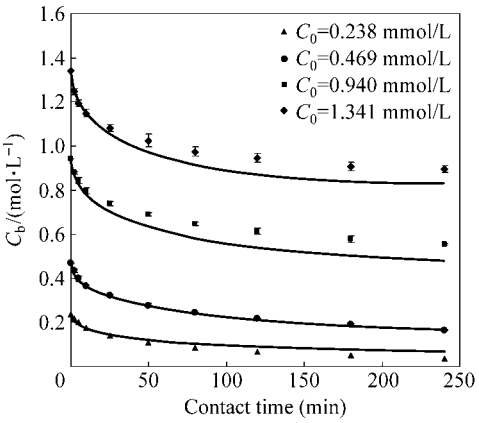

Fig. 3 Evolution of Pd(II) concentrations in the reservoir for various initial concentrations: adsorbent mass is 0.2 g (125-180 μm); recycle flow rate is 40 mL/min; C_b is the Pd(II) concentration measured from the reservoir at given times; solid lines calculated from the pore diffusion model (D_M = 8.33×10^{-6} cm^2/s, τ = 2.5).

The constant leaching of platinum chloride before the main breakthrough indicates that there are other stable chloro-platinum complexes in the solution that are not reactive to pyrazole ligands. Even though spectral studies for this effluent platinum solution have not been performed, likely species are mono-dissociated hydrogenhexachloroplatinate ($HPtCl^{6-}$) or hydrolyzed chloroplatinum complexes, as reported by Nachtigall and Artelt in their ion chromatography study[22]. The breakthrough of Au(III) chloride is less sharp than those of Pd(II) and Pt(IV) chlorides. This broader breakthrough is most likely due to longer concentration transition through the column. A sharp breakthrough of Pd(II) chloride occurs after 900 bed volumes (2.68 L). Substantially large gaps between these breakthroughs show the possibility of complete separation of these noble metal chlorides at moderate concentrations. In addition, the loaded metals can successfully be eluted by using less than 15 bed volumes of 0.25-0.50 mol/L thiourea in 0.1 mol/L solutions with high percentage recovery (95%-100%).

We are able to predict the breakthrough curves of Pd(II) and Au(III) of the column using the pore diffusion model for the sorption, parameter correlations, the Langmuir isotherm, and the mass balance for the column[23]. Also, the breakthrough curve for Pt(VI) can be calculated. These results are shown with the experimental data in Fig. 4.

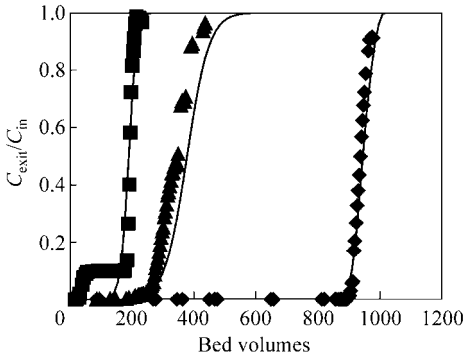

Fig. 4. Individual breakthrough curves of SOL-PzPs-BD-5 for Pd (◆), Pt (■), and Au(▲) at 2.0 mol/L HCl concentration: adsorbent mass is 2.0 g (125-180 μm); bed volume is 2.98 mL; flow rate is 1.0-1.1 mL/min; feed concentration (C_{in}) is 1.0 mmol/L; maximum loading is 1.27 mmol Pd/g, 0.28 mmol Pt/g, and 0.50 mmol Au/g; C_{exit} is the metal concentration at column exit; solid line presents the result of model prediction.

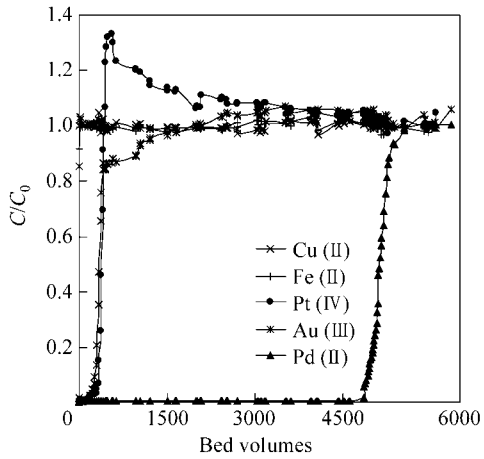

Fig. 5 Multimetal breakthrough curves in the column of SOL-PzPs-BD-5 (bed volume is 2.98 mL) in 2.0 mol/L HCl solution. Flow rate is 1.0-1.1 mL/min; feed solution composition: [Pd(II)], [Pt(IV)], and [Au(III)]: each 0.1 mmol/L; [Cu(II)] and [Fe(II)]: each 2.5 mmol/L; maximum loading is 0.77 mmol Pd/g, 0.00 mmol Pt/g, and 0.03 mmol Au/g.

A multi-metal breakthrough experiment is per formed to demonstrate the capability of SOL-PzPs-BD-5 to extract noble metals from highly concentrated transition metal solutions (Fig. 5). The breakthroughs of iron [Fe(II)] and copper [Cu(II)] from the SOL-PzPs-BD-5 column occur immediately after starting the experiment and indicate that this adsorbent has no reactivity for copper and iron. The breakthroughs of Au(III) and Pt(IV) chlorides occur simultaneously, and then these metals are displaced by the continual adsorption of Pd(II) chloride. Thus, this adsorbent has the strongest affinity for Pd(II) chloride[23].

2.2 Calix[4]arene crown functionalized organo-ceramic adsorbents for cesium separation

The structural properties of calix[4]arene-crown-6 and calix[4]arene-benzocrown-6 functional silica and titania adsorbents, as determined from nitrogen adsorption experiments, are shown in Table 3. The adsorbents show high surface areas and pore volumes, and mesopores, despite the incorporation of large hydrophobic calixarene ionophores. Only CC-Ti shows lower surface area and larger pore diameters, which can be attributed to the employment of a higher temperature during the aging/drying process (150℃ vs. 80 ℃). These structural properties can provide ease of transport of cesium ions through the pore channels thereby allowing rapid overall rate of adsorption. As shown in our previous studies[11,12], we also expect these adsorbents that the functional groups (calixarene derivative ionophores) are completely accessible to cesium ions for selective encapsulation, which is largely due to the employment of the sol-gel synthesis method in the preparation of these functional ceramics.

The distribution coefficient K_d increases with the increase in ligand densities, indicating a direct proportional relationship between K_d and the ligand density. In this study, the ligand density is not maximized as the purpose of this work is to determine the cesium ion extraction capabilities of the calix[4]arene derivative functional ceramics. A ligand

Table 3 Structural properties of cesium selective organo-ceramic adsorbents

Adsorbent	Matrix	Functionality	S_{BET} ($m^2 \cdot g^{-1}$)	d_p nm	V_p ($cm^3 \cdot g^{-1}$)
Calixol	Silica	Calix[4]arene-crown-6	648	2.5	0.41
CalixBC	Silica	Calix[4]arene-benzocrown-6	878	3.1	0.69
CC-Ti	Titania	Calix[4]arene-crown-6	7.8	49.0	0.18
CBC-Ti	Titania	Calix[4]arene-benzocrown-6	468	2.3	0.27

density of 10 mmol/g is demonstrated in Ref. [12]. Table 4 shows the distribution coefficients calculated from batch adsorption tests using simulants of acidic nuclear wastes. The lower K_d observed for this system compared to the system where only cesium ions are used implies the presence of competition between cesium ions and other cations such as sodium and potassium, which are known competitors for calix[4]arene crown cavities[24].

Table 4 Distribution coefficients (K_d) for Calixol and CalixBC from simulant solution

Adsorbent	$[Cs]_i$ (mg • L^{-1})	$[Cs]_{feed}$ (mg • L^{-1})	K_d (L • kg^{-1})
Calixol	1080	889	12.5
CalixBC	1141	982	9.5

Further evaluation of the silica-based OCAs through equilibrium studies are conducted for both materials along with a comparison with a material prepared through covalent attachment of calix[4]-crown-6 silane, as shown in Fig. 6. The maximum adsorption capacities for Calixol-50 and CalixBC-50 observed are 23 and 12 mg/g, respectively; however, according to the Langmuir type isotherms, slightly higher capacities are expected at higher cesium concentrations. As has been described through solvent extraction processes[25], cesium ions are encapsulated in calix[4]arene-crown-6 and calix[4]arene-benzocrown-6 on a 1:1 basis. The figure also demonstrates that the materials prepared by the sol-gel process show higher adsorption capacities compared to that prepared by the covalent attachment. This result also clearly demonstrates the ligand loading limitation of the immobilization method using mesoporous materials especially when the ligands are large in size.

The breakthrough curves for Calixol and CalixBC have been constructed and that for CalixBC is shown in Fig. 7. Both curves are sharp with similar breakthrough points and shapes under the same experimental conditions, indicating similar column performances for Calixol and CalixBC. The effluent concentration (as shown by the inset of the figure) reaches below 0.003 mg/L for CalixBC, even in the presence of high volumetric flow rates (0.28 mL/min). Such flow rate is permitted due to the high porosities of the materials and rapid adsorption kinetics. The

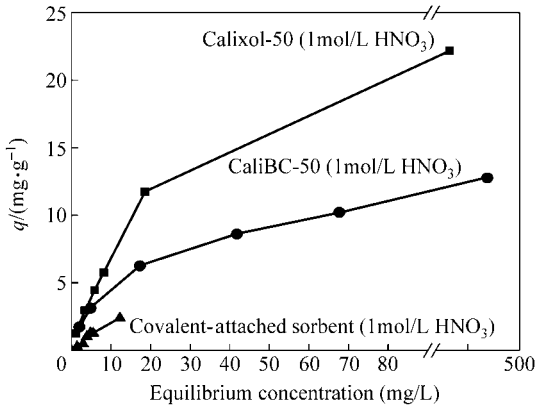

Fig. 6 Equilibrium isotherm for calixarene derivative functional materials; 1mol/L HNO_3, m = 0.1 g, V = 5 mL, contact time = 24 h.

materials can be regenerated by eluting the encapsulated cesium with dilute HCl solutions. The eluting efficiency using 0.01 mol/L HCl is found to be 90%.

Titania-based OCAs (CC-Ti and CBC-Ti) have been prepared and tested for cesium ion separation from highly alkaline solutions. These materials have calix[4]arene-crown and calix[4]arene-benzocrown groups incorporated in the titania matrices. Results demonstrate chemical stability of these materials in 2 mol/L NaOH solutions retaining the cesium adsorption capacity, and a potential application to alkaline nuclear waste separations.

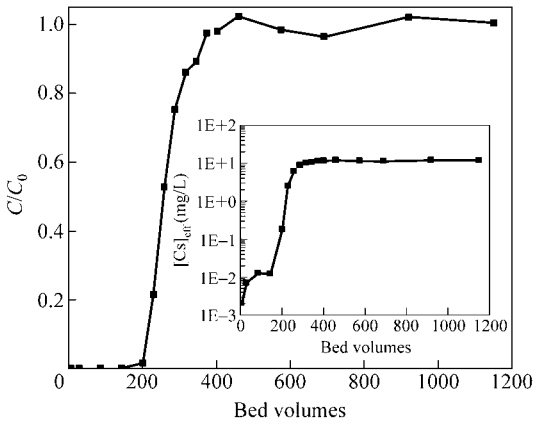

Fig. 7 Breakthrough curves for CalixBC; insets showing effluent concentrations; m=0.45 g, V=1000 mL, Q= 0.28 mL/min, $[Cs]_{feed}$ = 10 mg/L; bed volume is 0.87 mL; particle size range is 125-180 μm.

3 Conclusions

The organo-ceramic adsorbents functionalized with pyrazole ligands, SOL-PzPs-B-18, and SOL-PzPs-BD-5 are synthesized by sol-gel processing technology for

the separation of noble metals at high HCl concentrations. It is shown from this study that an appropriate hydrothermal treatment after gelation can alter pore structures of organo-ceramic adsorbents to give well-developed mesopores and consequently improve adsorption characteristics without sacrificing metal uptake capacities. Operational stability test for SOL-PzPs-BD-5 shows that this adsorbent has long-term stability over the repeated loading and regeneration in a packed column. Equilibrium studies show Langmuir type isotherms, and breakthrough curves show effluent concentrations as low as 0.003 mg/L in the extraction of cesium ions using calix[4]arene-crown and calix[4]arene-benzocrown functional silica- and titania-based-OACs. The silica- and titania-based OACs have applications to selective cesium separations from the U.S. Department of Energy's underground storage tanks, such as those located at the Idaho National Engineering and Environmental Laboratory, Savannah River Site, Hanford, and the Oak Ridge National Laboratory.

References

[1] Beck J S, Vartuli J C, Roth W J, Leonowicz M E, Kresge C T, Schmitt K D, Chu C T-W, Olson D H, Sheppard E W, McCullen S B, Higgins J B, Schlenker J L. *J. Am. Chem. Soc*., 1992, **114**: 10834.

[2] Alexandratos S D, Natesan S. *Macromolecules*, 2001, **34**: 206-210.

[3] Arena G, Casnati A, Contino A, Mirone L, Sciotto D, Ungaro R. *Chem. Commun*., 1996: 2277-2278.

[4] Nechifor A M, Philipse A P, de Jong F, van Duynhoven J P M, Egberink R J M, Reinhoudt D N. *Langmuir*, 1996, **12**: 3844-3854.

[5] Katz A, Da Costa P, Chun Pong Lam A, Notestein J M. *Chem. Mater*., 2002, **14**: 3364-3368.

[6] Lin Y, Fryxell G E, Wu H, Engelhard M. *Environ. Sci. Technol*., 2001, **35:** 3962-3966.

[7] Lee J S, Tavlarides L L. *Solvent Extraction and Ion Exchange*, 2002, **20**(3): 407-427.

[8] Tavlarides L L, Deorkar N V, Lee J S. US Pat., Appl. No. 09/573,304. Filed 5/18/2000.

[9] Lee J S, Gomez-Salazar S, Tavlarides L L. *Reactive and Functional Polymer*, 2001, **49**: 159-172.

[10] Gomez-Salazar S, Lee J S, Heydweiller J C, Tavlarides L L. *Ind. Eng. Chem. Res*., 2003, **42**(14): 3404-3412.

[11] Nam K H, Gomes-Salazar S, Tavlarides L L. *Ind. Eng. Chem. Res*., 2003, **42**(9): 1955-1964.

[12] Nam K H, Tavlarides L L. *Solvent Extr. Ion Exch*., 2003, **21**(6): 899-913.

[13] Trofimenko S. *Chemical Reviews*, 1972, **72**: 487-509.

[14] Saha N, Bhattacharyya D, Kar S K. *Inorganica Chimica Acta*, 1982, **67**: L37-L38.

[15] Govind B, Satyanarayana T, Veera Reddy K. *Polyhedron*, 1996, **15**: 1009-1022.

[16] Pronin V A, Usol'tseva M V, Shastina E N, Volkov A N, Seraya V I. *Zhurnal Neorganicheskoi Khimii*, 1974, **19**: 800-802.

[17] Pronin V A, Usol'tseva M V, Shastina E N, Volkov A N, Sokolyanskaya L V. *Zhurnal Analiticheskoi Khimii*, 1976, **31**: 1767-1769.

[18] du Preez, Knoetze J G H S E, Ravindran S. *Solvent Extraction and Ion Exchange*, 1999, **17**: 317-332.

[19] Ji H-F, Dabestani R, Brown G M, Hettich R L. *J. Chem. Soc., Perkin Trans*. 2001, **2**(2): 585-591.

[20] Casnati A, Pochini A, Ungaro R, Ugozolli F, Arnaud F, Fanni S, Schwing M-J, Egberink R J M, de Jong F, Reinhoudt N. *J. Am. Chem. Soc*., 1995, **117**: 2767-2777.

[21] Speier J L. *Adv. Organomet. Chem*., 1979, **17**: 407.

[22] Nachtigall D, Artelt S. *G. Wunsch. A*., 1997, **775**: 197-210.

[23] Lee J S, Tavlarides L L. *AIChE J*., 2005, **51**(10): 1-10.

[24] Sachleben R A, Urvoas A, Bryan J C, Haverlock T J, Hay B P, Moyer B A. *Chem. Commun*., 1999: 1751.

[25] Nam K H, Lee J S, Agarwal N, Tavlarides L L. *Ind. Eng. Chem. Res*., submitted.